Journal of South American Earth Sciences 63 (2015) 20–35

Contents lists available at ScienceDirect

Journal of South American Earth Sciences

journal homepage: www.elsevier.com/locate/jsames

Kaolinite, illite and quartz dissolution in the karstification of Paleozoic sandstones of the Furnas Formation, Paraná Basin, Southern Brazil☆

Mário Sérgio de Melo [a,*], Gilson Burigo Guimarães [a], Adilson Luiz Chinelatto [b], Paulo César Fonseca Giannini [c], Henrique Simão Pontes [a], Adriana Scoton Antonio Chinelatto [b], Daniel Atencio [c]

[a] UEPG – Departamento de Geociências, Ponta Grossa, PR, Brazil
[b] UEPG – Departamento de Engenharia de Materiais, Ponta Grossa, PR, Brazil
[c] Instituto de Geociências da USP, Rua do Lago 562, CEP 05508-080, São Paulo, SP, Brazil

ARTICLE INFO

Article history:
Received 8 January 2015
Received in revised form
18 June 2015
Accepted 29 June 2015
Available online 3 July 2015

Keywords:
Furnas Formation
Kaolinite dissolution
Quartz dissolution
Arenisation
Non-carbonate karst

ABSTRACT

Karstification processes in sandstones of the Furnas Formation, Silurian to Devonian of the Paraná Basin, have been described since the mid-twentieth century. However, some geologists still doubt the idea of true karst in sandstones. Studies carried out in the Campos Gerais region, Paraná State, Southern Brazil, aimed at investigating the nature of erosion processes in Furnas Formation and the role of the dissolution in the development of their notorious erosive features and underground cavities. These studies have led to the recognition of dissolution macro to micro features ('furnas', caves, ponds, sinks, ruiniform relief on cliffs and rocky surfaces, grain corrosion, speleothems, mineral reprecipitation and incrustation). The analysis (scanning electron microscopy, energy dispersive spectrometry and x-ray diffractometry) of sandstones and their alterites has indicated significant dissolution of clay cement along with discrete quartz grain dissolution. This mesodiagenetic cement (kaolinite and illite) is dissolved and reprecipitated as clay minerals with poorly developed crystallinity along with other minerals, such as variscite and minerals of the alunite supergroup, suggesting organic participation in the processes of dissolution and incrustation. The mineral reprecipitation usually forms centimetric speleothems, found in cavities and sheltered rocky surfaces. The cement dissolution associated with other factors (fractures, wet weather, strong hydraulic gradient, antiquity of the landforms) leads to the rock arenisation, the underground erosion and the appearance of the karst features. Carbonate rocks in the basement may locally be increasing the karst forms in the overlying Furnas Formation. The recognition of the karst character of the Furnas Formation sandstones has important implications in the management of underground water resources (increasingly exploited in the region), in the use of the unique geological heritage and in the prevention of geo-environmental accidents resulting from underground erosion phenomena.

1. Introduction

For decades the typical relief of the Paleozoic sandstones of the Furnas Formation in the Campos Gerais region, Southern Brazil, has suggested genesis from dissolution phenomena (Maack, 1946, 1956). Studies had already revealed wide variation in the production of groundwater from deep-drilled wells in the Furnas Formation (Maack, 1970), indicating that it is not a simple porous aquifer. More recent studies (Melo and Giannini, 2007; Melo et al., 2011) confirmed the importance of dissolution in the processes of surface and underground erosion in the sandstones. Several factors interact for such phenomena: the nature of the rock, sedimentary and brittle structures, scarped relief, antiquity of the rocks and relief and dominance of humid climates. An alternative interpretation for part of the erosive features developed in these sandstones has been postulated (Sallun Filho and Karmann, 2007), in which their origin is related to the influence of karst phenomena in the underlying rocks of the basement of the Paraná Basin (Proterozoic carbonate rocks of the Itaiacoca Group). However, this should not

☆ Research sponsored by the CNPq – Conselho Nacional de Desenvolvimento Científico e Tecnológico – process n° 477608/07-8.

* Corresponding author. UEPG-DEGEO, Av. Gal. Carlos Cavalcanti 4748, CEP 84.030-900, Ponta Grossa, PR, Brazil.
E-mail address: msmelo@uepg.br (M.S. Melo).

http://dx.doi.org/10.1016/j.jsames.2015.06.011
0895-9811/

be understood as a required factor for karst regional features and phenomena in the Paleozoic sandstones. They occur throughout the outcropping area of the Furnas Formation, whether or not carbonate rocks appear in the substrate.

In view of this controversy regarding the origin of the erosive features of the Furnas Formation, this study sought to highlight the role of the dissolution phenomena and resulting features in the sandstones. Macro erosion forms ('furnas', caves, ponds, sinks, ruiniform relief on cliffs and rocky surfaces) are relatively well described in the Furnas Formation, with the processes involved in their evolution extensively discussed (e.g. Maack, 1956; Soares, 1989; Melo et al., 1999; Melo and Giannini, 2007; Melo et al., 2011). Here, micro erosive features and other affiliates are described and their genesis integrated with the development of major features, aiming to understand the evolution of this particular geomorphic system as a non-carbonate karst system.

The recognition of the critical role of dissolution and that the Furnas Formation behaves like a real karst system with typical processes, landscapes and hydrodynamics implies social, educational, economic and scientific consequences: the Campos Gerais region urgently requires preservation policies for its natural and archaeological heritage, geo-environmental risk prevention, management of underground water resources, as well as educational activities for sustainability and paleoclimatic and paleoenvironmental research (Melo et al., 2011).

2. Geological and geomorphological overview

The Furnas Formation (Silurian-Devonian of the Paraná Basin) (Bergamaschi, 1999) is the predominant rock unit in the Campos Gerais region (Fig. 1). Its rocks are relatively resistant to weathering processes and support the Devonian Escarpment, a *cuesta* that separates the First from the Second Paraná Plateau (Fig. 2). The formation is up to 270 m thick in the study area and consists mainly of quartz sandstones, with the original composition ranging between quartz sandstones and subarkoses or even arkoses. The current quartz dominance results from diagenetic processes destroying the original feldspars (De Ros, 1998). The composition includes, among detrital minerals, quartz (97%), feldspars (1%), lithic fragments (1%) and micas (1%), with minor accessory minerals.

Grain size of quartz sandstones varies from fine sand to conglomeratic sand and mainly medium to coarse sand. Conglomerates and conglomeratic sandstones are common at the base of the unit, while towards the top intercalated silty and micaceous muddy layers become more frequent (Assine, 1996; De Ros, 1998; Lobato and Borghi, 2005). In thin section, the quartz grains usually appear with angular boundaries as a result of diagenetic overgrowth (De Ros, 1998; Melo and Giannini, 2007).

The diagenetic evolution of these quartz sandstones has involved various phenomena in several phases, including prior dissolution and reprecipitation by hot circulating fluids through fractures related to the mainly Mesozoic uplift and magmatism along the Ponta Grossa Arch region (De Ros, 1998). Macro and meso erosion features which may have originated at this time are apparently not observed nowadays. The features currently observed, whether they are the "furnas", the largest karst features in the area, or alveoli, runnels and other meso features in outcrops, are always related to processes and other associated features that indicate relatively recent development linked to the evolution of the current relief (Maack, 1956; Soares, 1989; Melo and Giannini, 2007).

Authigenic minerals are mainly quartz, as syntaxial overgrowth, and kaolinite and illite, as intergranular cement, with minor amounts of chlorite, albite, carbonate and anatase (Ramos and Formoso, 1975; De Ros, 1998).

Such diagenetic evolution leads to two characteristics of the Furnas Formation sandstones that greatly influence its erosion and weathering processes (De Ros, 1998; Melo et al., 1999; Melo and Giannini, 2007; Melo et al., 2011): relatively low average porosity (9%) and intense kaolinite cementation (up to more than 20%, with an average of 13%).

Furnas Formation rocks in the Campos Gerais region are heavily deformed by brittle structures (faults and fractures, sometimes with associated dykes), notably aligned in three directions (Zalán et al., 1991): (1) NE–SW (N50–70E), parallel to the old basement structures, repeatedly reactivated during the Phanerozoic; (2) NW–SE (N45–60W), parallel to the Ponta Grossa Arch axis, developed at the Mesozoic and related to the Gondwana break-up; (3) E–W, parallel to the ocean floor fractures and associated with the continental drift. All these structural directions have a key role in the groundwater flow and the evolution of erosive forms in the Furnas Formation rocks.

In the Campos Gerais region, the Furnas Formation usually lies directly on igneous and metamorphic Proterozoic to Cambrian rocks of the basement, among them the Itaiacoca Group, with carbonate metamorphic rocks. The Iapó Formation (Ordovician), discontinuous and thin basal unit of the Paraná Basin in the region, occasionally appears below the Furnas Formation. Overlaying the Furnas Formation appear either the Ponta Grossa Formation (Devonian), with gradual contacts (Assine et al., 1994), or heterogeneous rocks of the Itararé Group (Permian-Carboniferous), with erosive contacts. In some cases the Furnas Formation sandstones are confined between impermeable rocks of the basement beneath (granite batholiths, pelitic metasedimentary rocks), and the Ponta Grossa Formation above. A few artesian groundwater wells in the city of Ponta Grossa seem to be indicative of this local confinement. Elsewhere underlying karst and/or fractured rocks along shear zones constitute a very porous basement.

3. Data acquisition

Field surveys were conducted in outcrops and underground cavities (caves, sinkholes, grikes), as well as in artificial exposures. The selection of study sites (Table 1) resulted from previous studies (Melo et al., 1999, 2005; Melo and Giannini, 2007; Melo et al., 2011) that indicated key situations linking information from micro to macro scale. Rock samples mainly with evidence of dissolution and recrystallization processes were collected in the majority of these sites (Table 1). The sampling targeted three main kinds of surface features: speleothems in sandstone caves or vugs (CC-01 to CC-06, FU-33E); hardening incrustations along subvertical fractures and rock shelters (FU-16E, FU-35) or outcrop wall (FU-25A); botryoidal crusts on cliffs (FU-33C). The sample PS-23 was collected in an outcropping sandstone without apparent surface dissolution or precipitation. These geological sets of samples were considered to be representative of the processes and products of dissolution and reprecipitation identifiable in the scale of the grains of the sandstones, whose microanalysis can support the understanding of the development of greater forms.

The samples were studied by scanning electron microscopy (SEM), energy dispersive spectrometry (EDS) and x-ray diffractometry (XRD) for analysis of the packing and composition of sandstones and derived materials (incrustations, speleothems) and interpretation of the processes involved. *In natura* millimeter fragments of rock samples were used for SEM and EDS analyses on a Shimadzu equipment model SSX-550. The samples were previously dried (24 h at a temperature of about 40 °C) and then metalised with gold. The electron micrographs and EDS spectra were

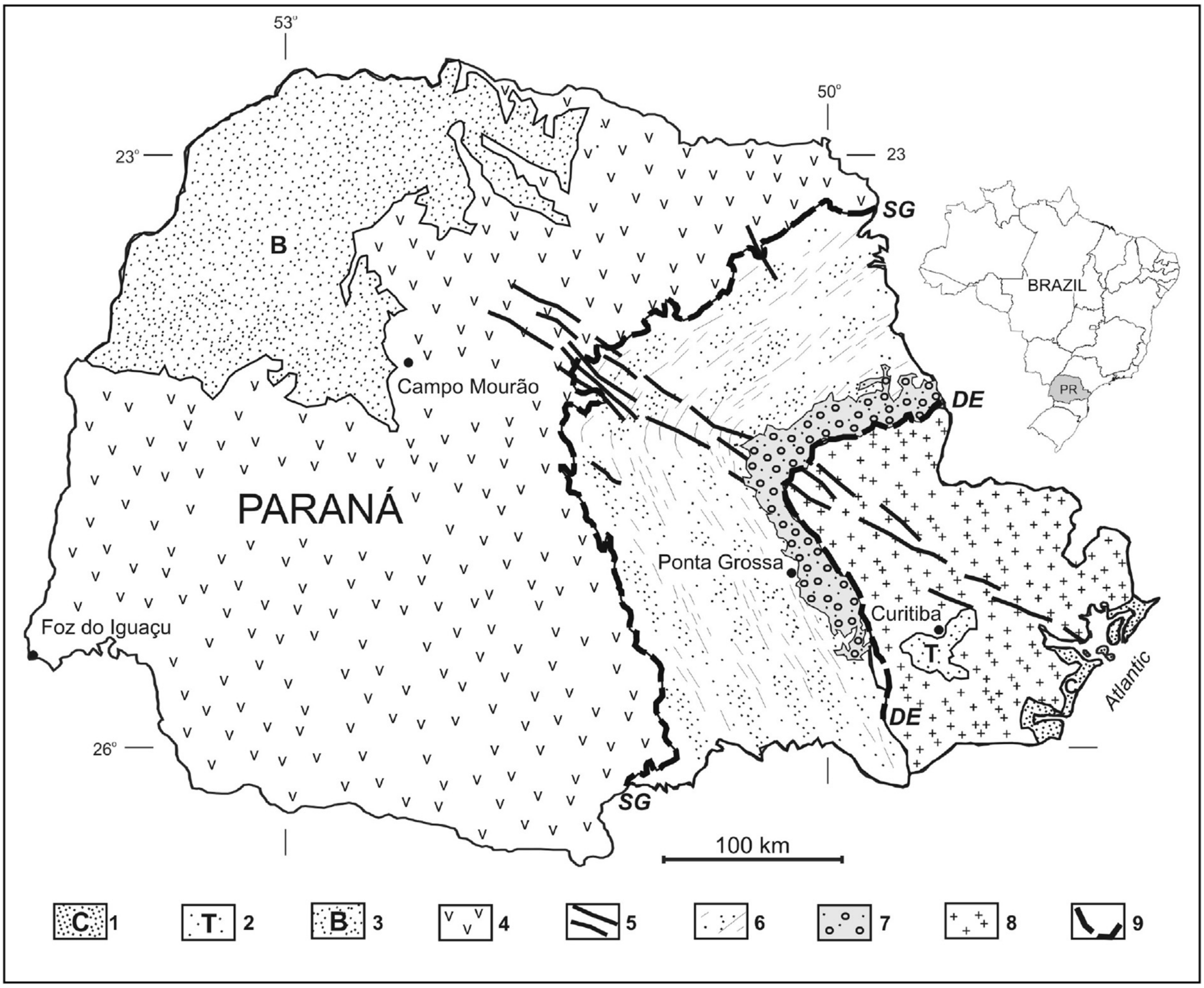

Fig. 1. Simplified geological map of the State of Paraná showing the outcropping area of the Furnas Formation. 1: Cenozoic sediments of the coastal plain; 2: Cenozoic continental sediments of the Curitiba Tertiary Basin; 3: Bauru and Caiuá Groups (Cretaceous); 4: lava flows of the Serra Geral Formation (Cretaceous); 5: main Cretaceous dykes parallel to the axis of the Ponta Grossa Arch; 6: Paleozoic and Mesozoic sedimentary units of the Paraná Basin (younger than the Furnas Formation); 7: Furnas Formation (Silurian-Devonian); 8: Precambrian Basement; 9: Escarpments (*DE*: Devonian Escarpment; *SG*: Serra Geral). Based on Maack (1948), Biondi et al. (1989) and Mineropar (2006).

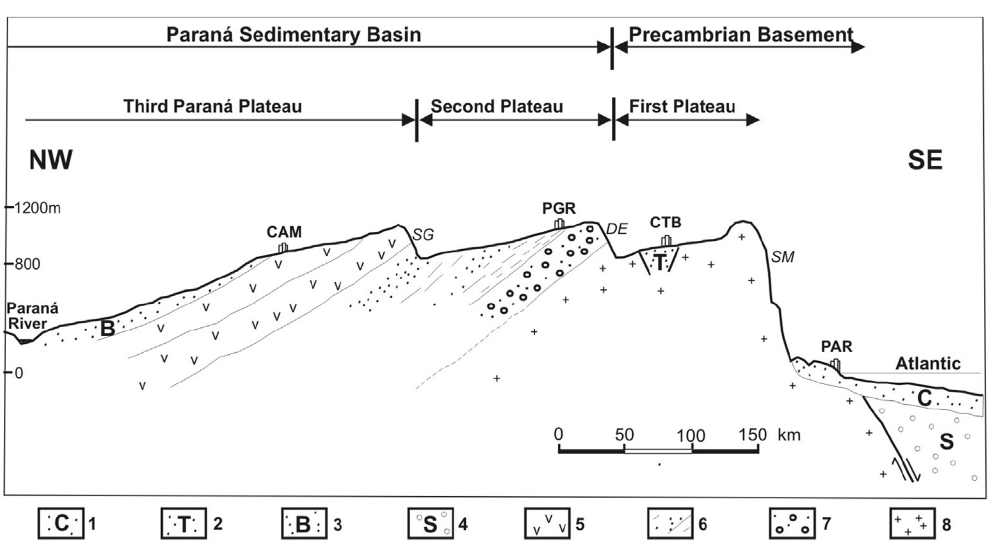

Fig. 2. Schematic geological structure of the relief of the Paraná State (section SE–NW crossing the entire Paraná State). 1: Cenozoic sediments of the coastal plain and the Continental Shelf; 2: Cenozoic continental sediments of the Curitiba Tertiary Basin; 3: Bauru and Caiuá Groups (Cretaceous); 4: Santos Basin (Mesozoic); 5: lava flows of the Serra Geral Formation (Cretaceous); 6: Paleozoic and Mesozoic sedimentary units of the Paraná Basin (younger than the Furnas Formation); 7: Furnas Formation (Silurian-Devonian); 8: Precambrian Basement. Cities: PAR: Paranaguá; CTB: Curitiba; PGR: Ponta Grossa; CAM: Campo Mourão. Escarpments: *SM*: Serra do Mar; *DE*: Devonian Escarpment; *SG*: Serra Geral.

Table 1
UTM coordinates (zone 22 J) of locations mentioned in the text and/or where samples analyzed in this paper (marked with*) were collected.

Sample	N	E	Altitude (m)	Location
CC-01 to CC-06*	7.231.165	596.161	951	Chaminé Cave
FU-16*	7.283.945	575.704	851	Guartelá Canyon
FU-25*	7.282.781	575.837	997	Guartelá Canyon, 'Seu Olímpio' smallholding
FU-27	7.282.895	574.756	1048	Guartelá Canyon (rain's rock shelter)
FU-28	7.295.387	597.584	1048	Trail to the Paulina Fall
FU-29	7.295.270	597.725	1067	Trail to the Paulina Fall
FU-30*	7.295.183	597.850	1088	Trail to the Paulina Fall
FU-33*	7.213.812	604.463	930	Macarrão climbing area
FU-35*	7.282.636	576.032	988	Lapa (*Rock Shelter*) Ponciano
FU-36*	7.218.306	605.179	1035	Furnas Gêmeas (*Twin Sinkholes*)
GU-05	7.283.163	575.770	999	Portal de Pedra (*Stone Gateway*), Guartelá Canyon
GU-06	7.282.722	576.062	985	Cabeça de Camelo (*Camel Head*), near Lapa Ponciano
GU-09*	7.281.768	576.889	1028	Lapa Floriano
PS-129	7.296.177	589.457	1003	Guaricanga River (left margin)
PS-23*	7.277.656	584.719	1185	Uphill trail to the Mucambo Farm
SU-05*	7.211.935	603.676	878	Shelter in the Quebra-Perna Sink (right margin)
SU-07*	7.211.804	603.569	902	Shelter in the Quebra-Perna Sink (left margin)
–	7.215.653	603.999	915	Buraco do Padre (*Priest's Hole*)
–	7.303.277	608.695	1087	Furna das Curucacas (*Curucacas Sinkhole*)
–	7.177.488	629.311	1039	Furna do Tamanduá 1 (*Tamanduá I Sinkhole*)
–	7.175.143	627.879	982	Furna do Tamanduá 2 (*Tamanduá II Sinkhole*)

compared with a specific atlas (Welton, 1984) to support the identification of minerals and their origin. The XRD analyses were held in a Shimadzu diffractometer XRD-6000, under the following conditions: 2θ ranging from 5 to 90°, scan rate of 2°/min and radiation of Cu-K_{α}. Mineral identification was carried out using the software *Search Match Version 3.01 (Shimadzu)*.

4. Results

Results are shown in Figs. 3–11 where outcrop features (hardening incrustations, speleothems, botryoidal crusts) are related to SEM images and EDS spectra.

The common characteristics of the sandstone samples (Figs. 3–6, 11) are the apparently euhedral to subhedral quartz grains sometimes with corroded surfaces (Figs. 3B, 5C, 11C), which could be attributed to overgrowth, and the kaolinite booklets (Figs. 3E, 4E, 5D, 6G, 11D). Hard and botryoidal crusts are characterized by cryptocrystalline phyllosilicates (kaolinite and/or illite; Fig. 5G) or silica cements (Fig. 6E). A common feature of the speleothem samples is the presence of cryptocrystalline to amorphous silica (Figs. 4G, 8C, 9H, 10D).

Quartz overgrowth appears covered by kaolinite booklets (Fig. 3B). The kaolinite booklets are up to 50 μm thick and formed of pseudo-hexagonal sheets exceeding 10 μm (Figs. 3E, 4E, 5D, 6G, 8G, 11D and G). Well crystallized illite is found besides kaolinite booklets in some of the samples containing the original sandstone (Figs. 3G and 5E). It occurs as sheets up to 10 μm wide with filiform terminations more or less developed (Figs. 3G and 5E respectively).

Signs of corrosion and dismantling on kaolinite plates were seen in part of the SEM images of crust samples (Fig. 6C), including partial alteration to illite (Fig. 7E and F). Corrosion of illite was detected in a speleothem sample (Fig. 10H).

The cryptocrystalline kaolinite was found in speleothem samples (CC-06, CC-01, CC-05) as up to 4 μm irregular and subparallel plates, partially coalesced (Figs. 4G, 10A and F). The cryptocrystalline illite occurs in a sample of hardening incrustation (FU-16 E) as fibers and lamellae up to 6 μm wide (Fig. 5G).

Cryptocrystalline to amorphous silica (opal and other forms) appears in speleothem samples (FU-33E, CC-02), and in two incrustation samples (FU-25A, FU-35). In the SEM images, this silica can show the following forms: cylindrical or oblate batons up to 5 μm long with rounded terminations (Fig. 6F); globules less than 3 μm (Figs. 6E and 9H); massive between kaolinite plates (Fig. 8G); and rough film coating kaolinite polygonal plates (Fig. 11G). Sometimes globules occur as aggregates of spongy aspect (Fig. 9H).

In addition to kaolinite, illite and silica, other minerals such as Fe oxides and hydroxides, variscite or minerals within the alunite supergroup also appear (Figs. 7G and 11F). They usually occur in negligible amounts, only having expression as rock constituents in some speleothems and incrustations (Fig. 7B and C).

5. Discussion

The processes and features observed in the sandstones of the Furnas Formation have been compared to karstic phenomena since the 1940's (Maack, 1946). Other authors (Bigarella et al., 1994; Sallun Filho and Karmann, 2007) argue that alternative factors (mechanical erosion, karst in the basement of the Paraná Basin) would be responsible for the erosive features and underground cavities seen in the Paleozoic sandstones. In view of this controversy and of the enormous consequences of the recognition of a true karst system in the Furnas Formation for sustainable regional management, the following discussion will focus on these ideas.

5.1. Furnas Formation sandstones: diagenetic processes, mineral dissolution and associated features

Diagenetic history of the Furnas Formation sandstones can be roughly divided into three phases: Paleozoic eodiagenesis resulting from processes connected with the sedimentary burial; Mesozoic mesodiagenesis associated with the intense magmatic activity in the Paraná Basin; Cenozoic telodiagenesis related to the regional uplift, weathering and erosion from the Paleogene (De Ros, 1998; Melo and Giannini, 2007).

Syntaxial quartz overgrowth in the Furnas sandstones is identified by the large number of quartz grains apparently euhedral to subhedral (Figs. 3C, 5C, 11E) or juxtaposed by planar contacts (Melo and Giannini, 2007). It is one of the main processes of cement generation in the diagenetic history of the Furnas Formation. The quartz overgrowth preceded the formation of kaolinite booklets, resulting in well-formed faces coated by the kaolinite (Fig. 3C), but there is evidence that it also followed it (Fig. 6G), in accordance with previous conclusions regarding the existence of at least two phases of quartz cementation (De Ros, 1998). Considering that well

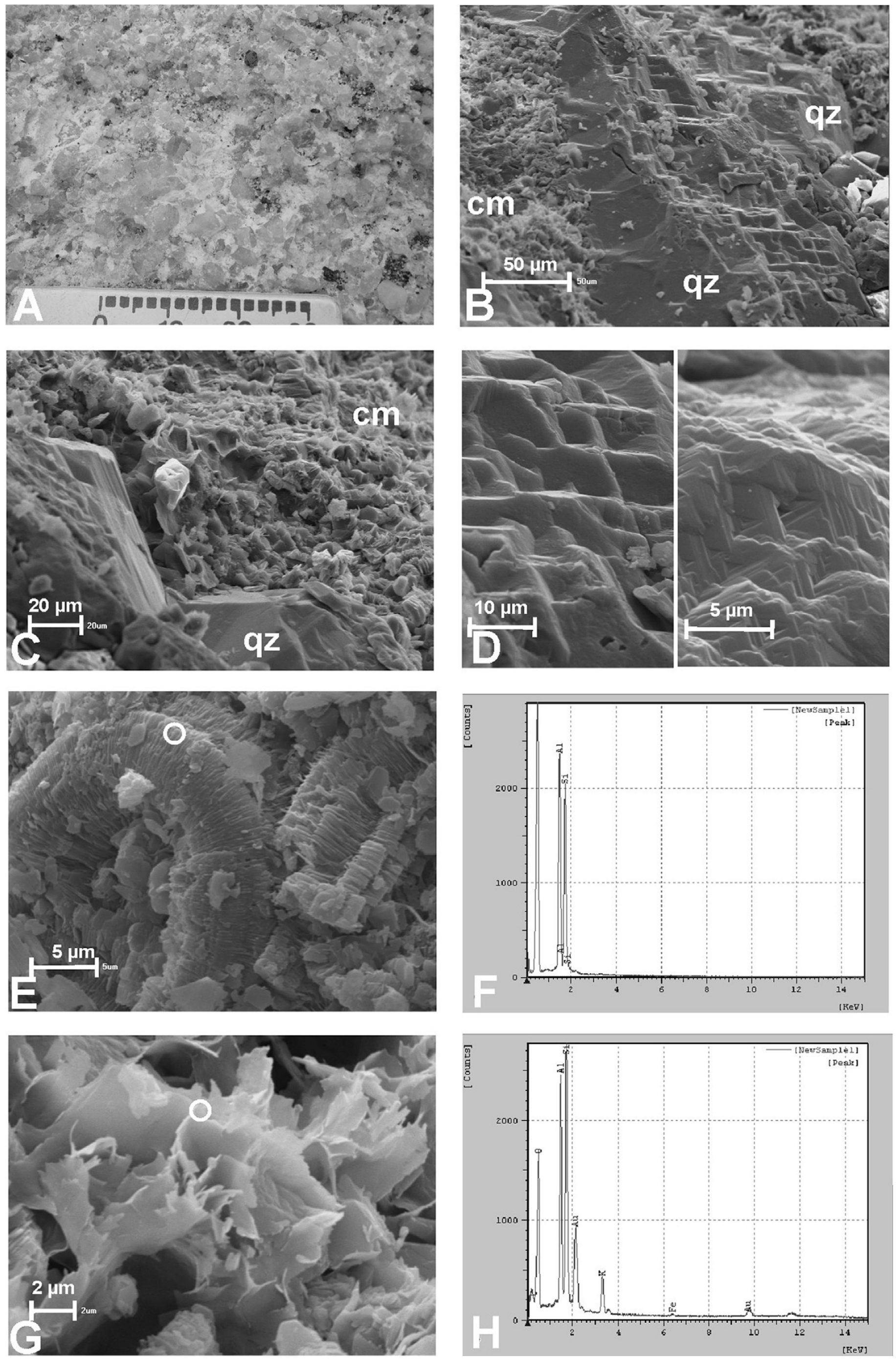

Fig. 3. Sample PS-23, view of the Furnas Sandstone in a rock exposure on a road slope. A: quartz grains surrounded by clear kaolinitic cement (scale in mm); B: SEM image showing quartz grain partially corroded (qz) surrounded by cement (cm); C: detail of quartz grain with euhedral faces; D: two details of corroded faces of quartz grains; E: booklets of mesodiagenetic kaolinite; F: EDS of the kaolinite in E; G: mesodiagenetic illite sheets; H: EDS of the illite in G (the white circles in E and G mark center of electron beam with 1 µm of radius used in the EDS).

crystallized kaolinite booklets, like these shown in this paper (Figs. 3E, 4E, 5D, 6G, 8G, 11D and G) are in general typically mesodiagenetic, the relationship between quartz overgrowth and these booklets leads to the conclusion that the overgrowth was formed during eodiagenesis and mesodiagenesis, along with the formation of kaolinite in mesodiagenesis.

Presumed illitization of kaolinite crystals (Fig. 7E and F) can be attributed, as argued by De Ros (1998), to the destruction of feldspars by meteoric water. Dissolution and kaolinization of detrital feldspars once present in the sandstones of the Furnas Formation are processes previously described and shown in detail (De Ros, 1998; Melo et al., 1999; Melo and Giannini, 2007).

The formation of well crystallized illite (Figs. 3G and 5E) seems to be penecontemporaneous to the kaolinite formation. De Ros (1998), supported by K/Ar dating, believes that some illite may result from illitization of kaolinite during the Mesozoic magmatism in the Paraná Basin. In this case, the illite's potassium would come from potassic feldspar transformation.

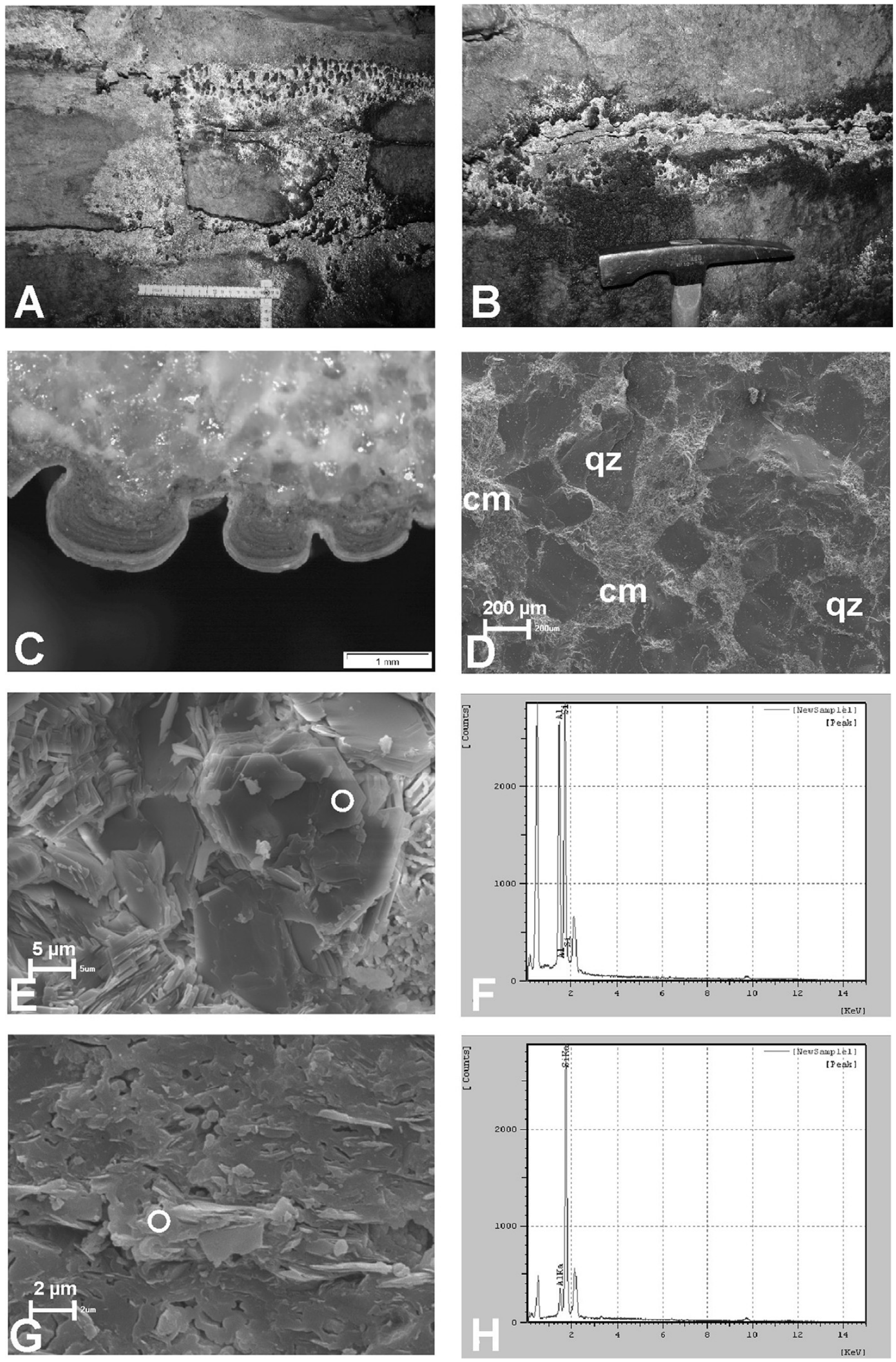

Fig. 4. Sample CC-06, from inner wall of the Chaminé Cave, with small speleothems. A: general view of the wall. B: speleothems locally with net structural control. C: stereo microscope image of sandstone and speleothems; D: SEM image of the sandstone showing quartz grains (qz), some with planar faces (apparently euhedral and subhedral) due to overgrowth, and cement (cm); E: detail of the cement in D; F: EDS of the cement, indicating that it is mesodiagenetic kaolinite; G: SEM image of the speleothem in C; H: EDS of the speleothem, indicating the presence of cryptocrystalline silica with little telodiagenetic kaolinite (the white circles in E and G mark the center of electron beam with 1 µm of radius used in the EDS).

Quartz corrosion previously mentioned in the literature (De Ros, 1998; Melo et al., 1999; Melo and Giannini, 2007) is visible here in several samples (Figs. 3B and D, 5C, 11C). Sample PS-23 (Fig. 3) shows corroded quartz overgrowth with abundant well crystallized kaolinite, suggesting some corrosion prior to the kaolinite mesodiagenesis. The widespread occurrence of corroded quartz overgrowth and the presence of cryptocrystalline to amorphous silica (Figs. 4G, 6F and G, 8C and G, 9H, 10D) point to the quartz dissolution as the source of part of this silica.

Kaolinite dissolution, previously referred to by Melo and Giannini (2007), is here indicated by corroded mesodiagenetic sheets (Fig. 6C), surface incrustations (Fig. 12F) and speleothems (Fig. 4C and G, 10A and F) of cryptocrystalline kaolinite, interpreted as telodiagenetic.

Illite dissolution is indicated by the presence of well formed crystals (Figs. 3G and 5E), contrasting with sheets with corroded aspect (Fig. 10H) and agglomerates with massive aspect (Fig. 5G), the latter interpreted as telodiagenetic.

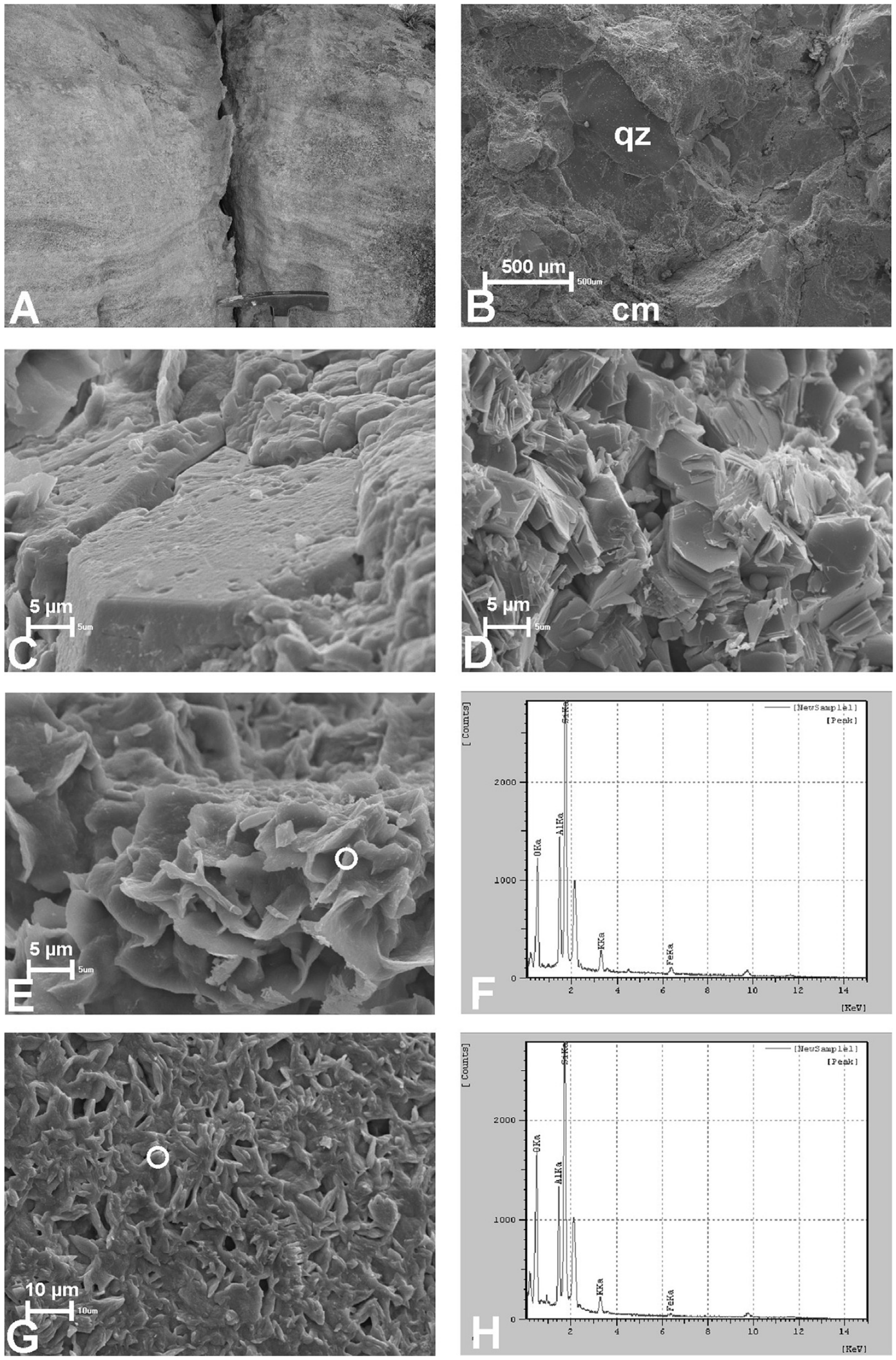

Fig. 5. Sample FU-16E, hardening incrustation along subvertical fracture in the Furnas Sandstone. A: outcrop view of the fracture with hardened crust. B: SEM image of the sandstone showing quartz grains (qz) and abundant intergranular cement (cm); C: detail of corroded surface of euhedral quartz grains; D: well crystallized kaolinite (mesodiagenetic) in the cement in B; E: well crystallized illite (mesodiagenetic) in the cement in B; F: EDS of the illite in E; G: poorly crystallized illite (telodiagenetic); H: EDS of the illite in G (the white circles in G and E mark the center of electron beam with 1 µm of radius used in the EDS).

Cryptocrystalline to amorphous silica (opal and other forms, Figs. 4G, 6E and F, 8C and G, 9C and H) derives from quartz dissolution and other processes, such as kaolinite and feldspar transformations (De Ros, 1998). This silica occurs as one of the main constituents of the centimeter to decimeter long speleothems (Figs. 4A–C, 8A and B, 9A, 10C and E), which strengthens its interpretation as a telodiagenetic product.

Other minerals such as iron oxides and hydroxides, variscite or minerals within the alunite supergroup can also be included among the telodiagenetic products (Figs. 7G and 11F), considering their association with speleothems and incrustations (Fig. 7B and C). Alunite has also been identified within opaline speleothems on quartz sandstone by Wray (2011), who believes that was the first report of such an occurrence.

SEM images often show porosity associated with telodiagenetic minerals formed mainly at the expense of feldspar (De Ros, 1998), quartz and well crystallized kaolinite and illite (Figs. 6F, 7G, 9B and C, 10D, 11E). Secondary porosity resulting from the removal of

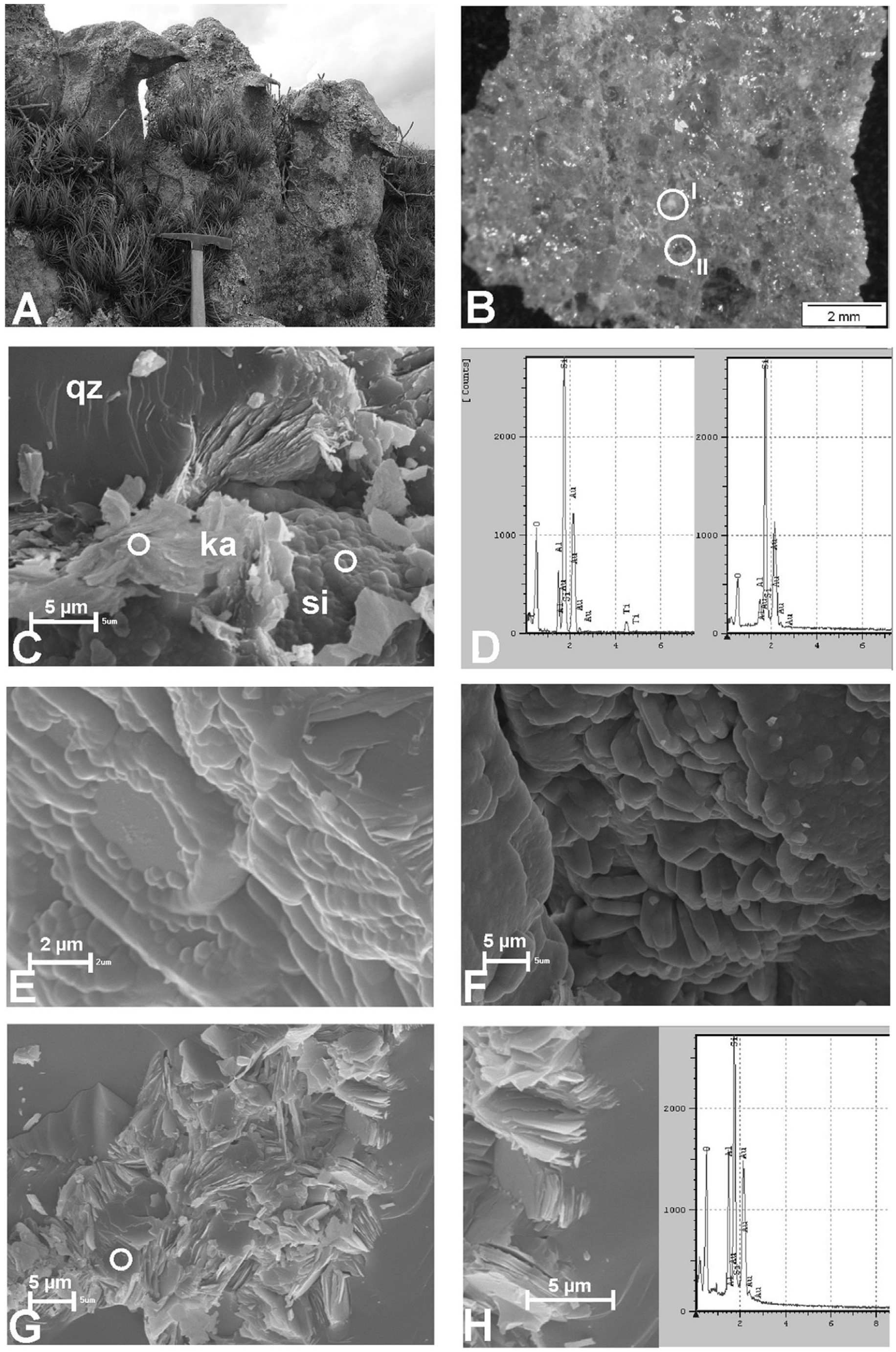

Fig. 6. Sample FU-25A, hardened surface in sandstone outcrop. A: outcrop view with surface saliences indicating hardening; B: stereo microscope image of the sandstone showing quartz grains and light saccharoidal (I) or dark caramel (II) cement; C: SEM image of the light saccharoidal cement (B–I), showing quartz grain (qz), corroded sheets of kaolinite (ka) and globular silica (si); D: EDS of the kaolinite sheets (left) and globular silica (right) in C; E: SEM image of the globular silica on kaolinite; F: baton-like silica; G: SEM image of the dark caramel cement (B-II), showing quartz grains with mesodiagenetic kaolinite and quartz overgrowth covering the kaolinite; H: detail of the overgrowth of quartz recovering kaolinite in G (left) and EDS of the kaolinite in G (right) (the white circles in C and G mark the center of electron beam with 1 μm of radius used in the EDS).

mesodiagenetic kaolinite is clearly visible in thin sections analysis by optical microscopy (Melo and Giannini, 2007). Both alteration and removal of the cement suggest weakening of intergranular cohesion, which favors the releasing of framework grains and, therefore, arenisation (Young et al., 2009).

Telodiagenetic processes described above have resulted in the formation of exfoliations (Fig. 12B and E), incrustations (Figs. 7B and C, 12F) and speleothems (Figs. 4A–C, 8A, 9A, 10C and E). These are small scale features indicative of dissolution and reprecipitation processes of minerals in the Furnas Formation sandstones. Sometimes exfoliations with telodiagenetic kaolinite affect rock paintings by prehistoric Indians (Fig. 12E), indicating that the dissolution and reprecipitation are younger than the paintings.

Based on the results and discussions above, Table 2 presents the main post-depositional processes responsible for eo, meso and telodiagenetic transformations identified in the Furnas Formation,

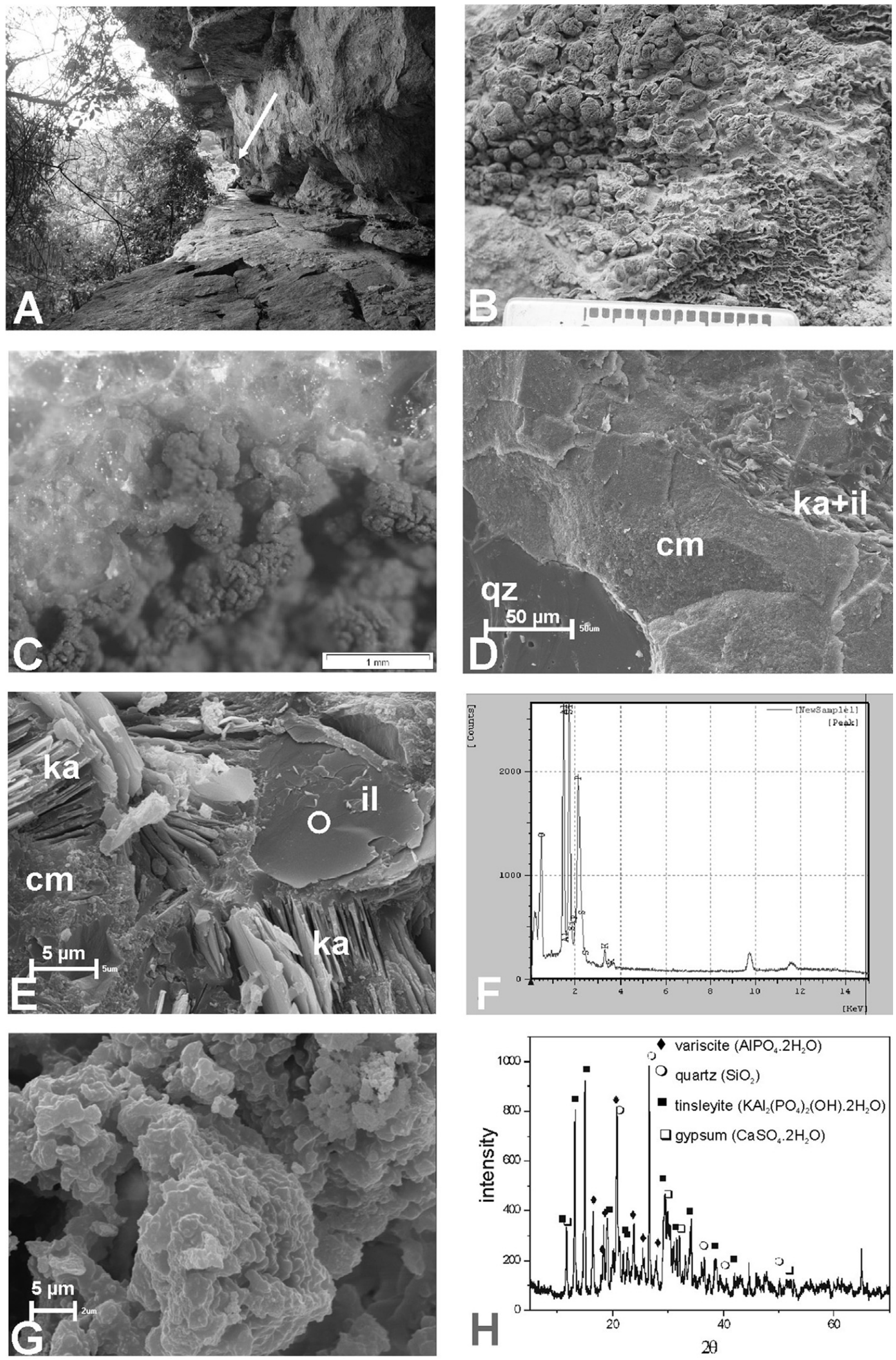

Fig. 7. Sample FU-33C, fringed and botryoidal incrustation in cliffs and rock shelters. A: shelter in the rock wall (arrow indicates seated man); B: detail of the botryoidal and fringed incrustations on the surface of the sandstone (scale in mm); C: stereo microscope image of the incrustations on the sandstone; D: SEM image showing quartz grain (qz), kaolinite and illite sheets (ka + il) enveloped in massive cement (cm); E: SEM image (detail of D) showing partially corroded sheets of illite (Il) and kaolinite (ka) and massive cement (cm); F: EDS of the illite in E, probably resulting from illitization of the kaolinite; G: SEM image of the massive cement in D and E; H: XRD of the incrustations in B suggesting the presence of variscite ($AlPO_4.2H_2O$), tinsleyite ($KAl_2(PO_4)_2(OH).2H_2O$), gypsum ($CaSO_4.2H_2O$), and quartz (the white circle in E marks the center of electron beam with 1 µm of radius used in the EDS).

the last of which includes dissolution and karstification phenomena. Mechanical compaction, not directly observed here, is mainly indicated by broken quartz grains and deformation of micaceous minerals (De Ros, 1998).

Telodiagenetic products are mostly preserved in the rock walls protected from the direct action of more aggressive weathering agents (rainfall, solar incidence, dew, organisms), as is the case with natural shelters (Figs. 7A, 11A, 12D). Especially at these places submetric features can be developed, such as alveoli (Fig. 12A, B and G). Runnels (or *karren*, Fig. 12C) and ruiniform reliefs (Figs. 6A and 11A) may develop on surfaces where rainwater runs off.

Several factors influence the efficiency of the mineral transformation processes in the Furnas Formation rocks. Sandstone grain size prevails, controlling the cement proportion against the

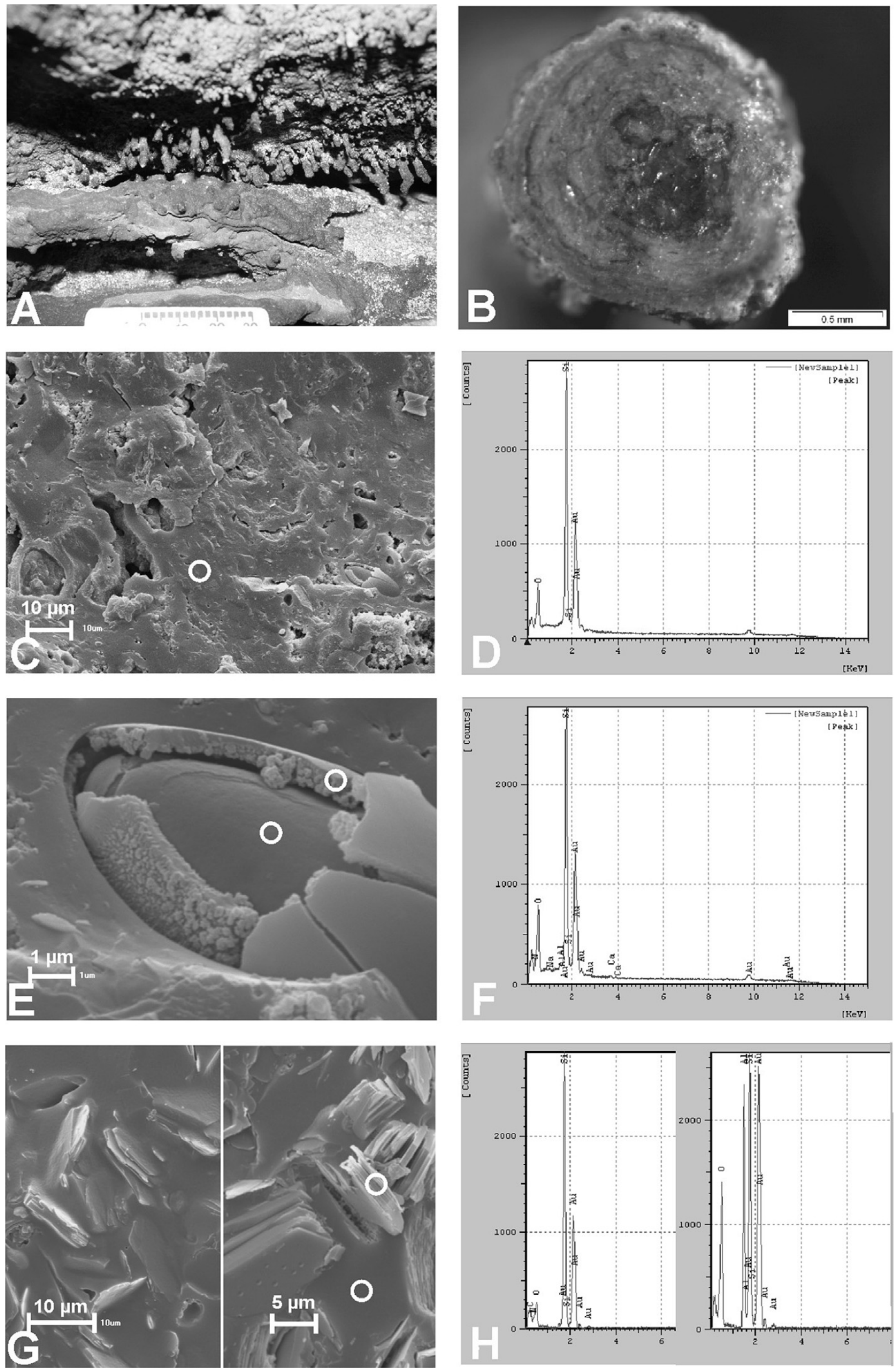

Fig. 8. Sample FU-33E, centimetric speleothems in cavity in rock wall. A: speleothems (scale in mm); B: cross-section of speleothem showing concentric arrangement; C: SEM image of outer edge of the speleothem in B; D: EDS of C, indicating that it is silica; E: detail of C showing microorganism structure; F: EDS of E indicating that it is essentially silica; G: two SEM images of kaolinite sheets (mesodiagentic) covered by amorphous material; H: EDS of the amorphous material in G indicating that it is silica (left) and EDS of the sheets in G, indicating that it is kaolinite (right) (the white circles in C, E and G mark the center of electron beam with 1 μm of radius used in the EDS).

framework components. Coarser sandstones develop erosion features more strongly (and supposedly faster) than rocks with finer textures (Fig. 12G and H).

Biological activity could be enhancing the dissolution and reprecipitation processes. Remains of organisms (Fig. 8C and E) and compounds such as variscite ($AlPO_4.2H_2O$), crandallite ($CaAl_3(PO_4)_2(OH)_5.H_2O$) (Melo and Giannini, 2007) and others containing phosphorous and sulfur in the speleothems and incrustations (Figs. 7H and 11F) suggest an organic influence on their geomorphic evolution. However, a mere trapping between mineral layers is not yet to be discarded, as discussed by Willems et al. (2002).

5.2. Dissolution in the Furnas Formation

The sandstones of the Furnas Formation show singular landforms indicative of combined action of dissolution and mechanic erosion: the furnas (collapsed hollows), ponds, wet and dry depressions, sinkholes, tunnels, grykes, alveolus, ruiniform relief and

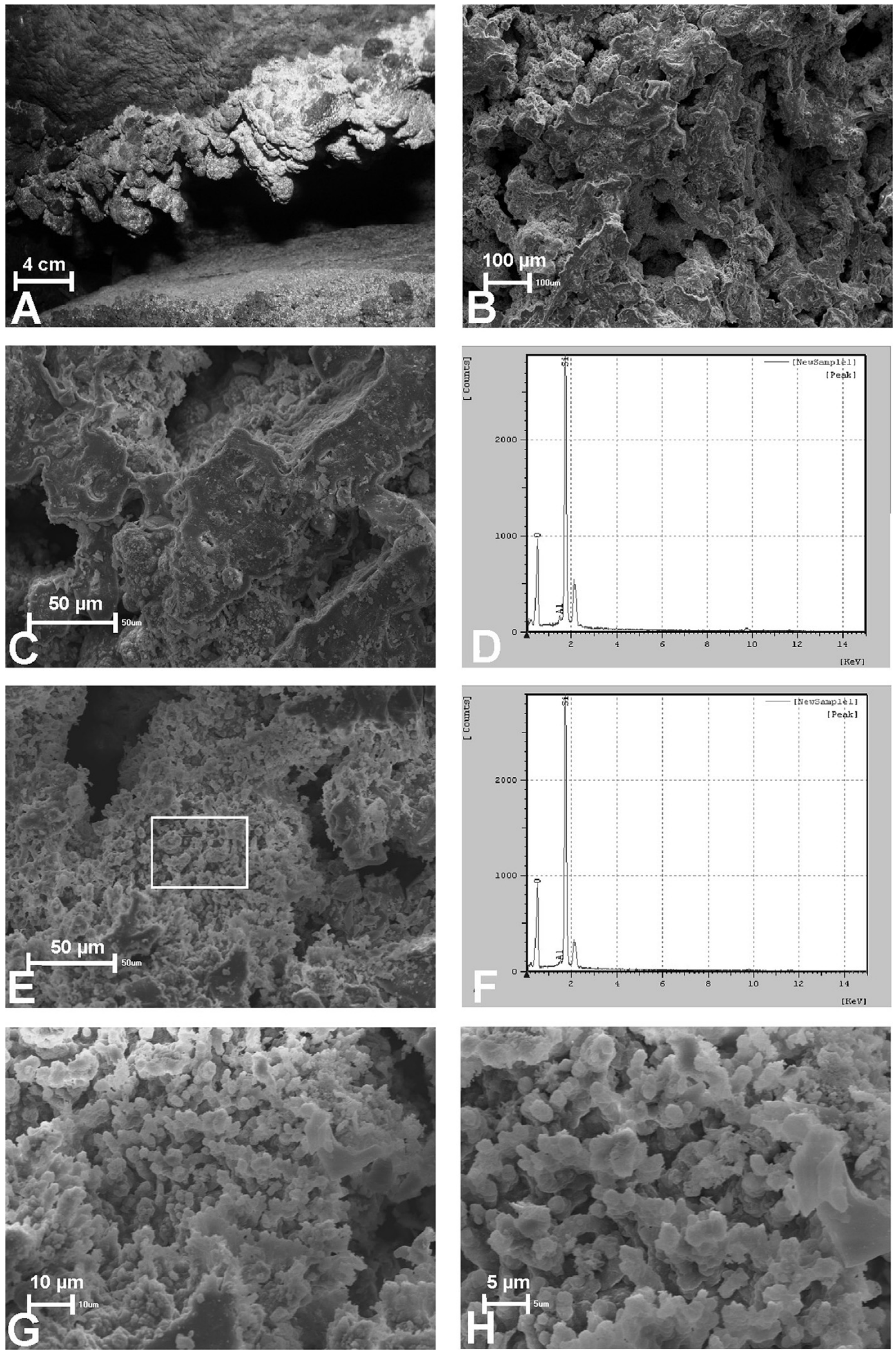

Fig. 9. Sample CC-02, speleothems in the Chaminé Cave. A: view of the speleothems; B: SEM image showing porous structure of the speleothems; C: detail of B showing massive areas and roughened pores; D: EDS of massive area in C indicating that it is silica; E: SEM image of the roughened area in C; F: EDS of the roughened area delimited by the rectangle in E indicating that it is silica; G: detail of E showing globular agglomerate of amorphous silica; H: detail of G.

secondary features as tafoni, grottoes, runnels, dissolution pans, anastomosing tunnels and columns (Maack, 1956; Melo and Giannini, 2007; Melo et al., 2011).

The furnas, interpreted as collapsed dolines up to 111 m deep (Maack, 1956; Soares, 1989), are the main evidence of the existence of underground cavities in the area of the Furnas Formation. Certain furnas could also be interpreted as the result of underlying carbonate karst (Maack, 1956; Sallun Filho and Karmann, 2007). However, at least in one place (Furna das Curucacas, 33 m deep, see Table 1) there are no known carbonate rocks that could cause the underlying karst. At other places (furnas Tamanduá I, 35 m deep and Tamanduá II, 26 m deep) the existence of underlying carbonate rocks is uncertain. Where underlying carbonate karst is refused the furnas should be interpreted as collapse over underground erosion cavities in the Furnas Formation sandstones developed mainly in the places where brittle structures intersect (Soares, 1989; Melo and Giannini, 2007).

The evidences described in Melo and Giannini (2007) and detailed in this paper suggest that a critical erosion process in the Furnas Sandstone is the dissolution of the kaolinite cement, the

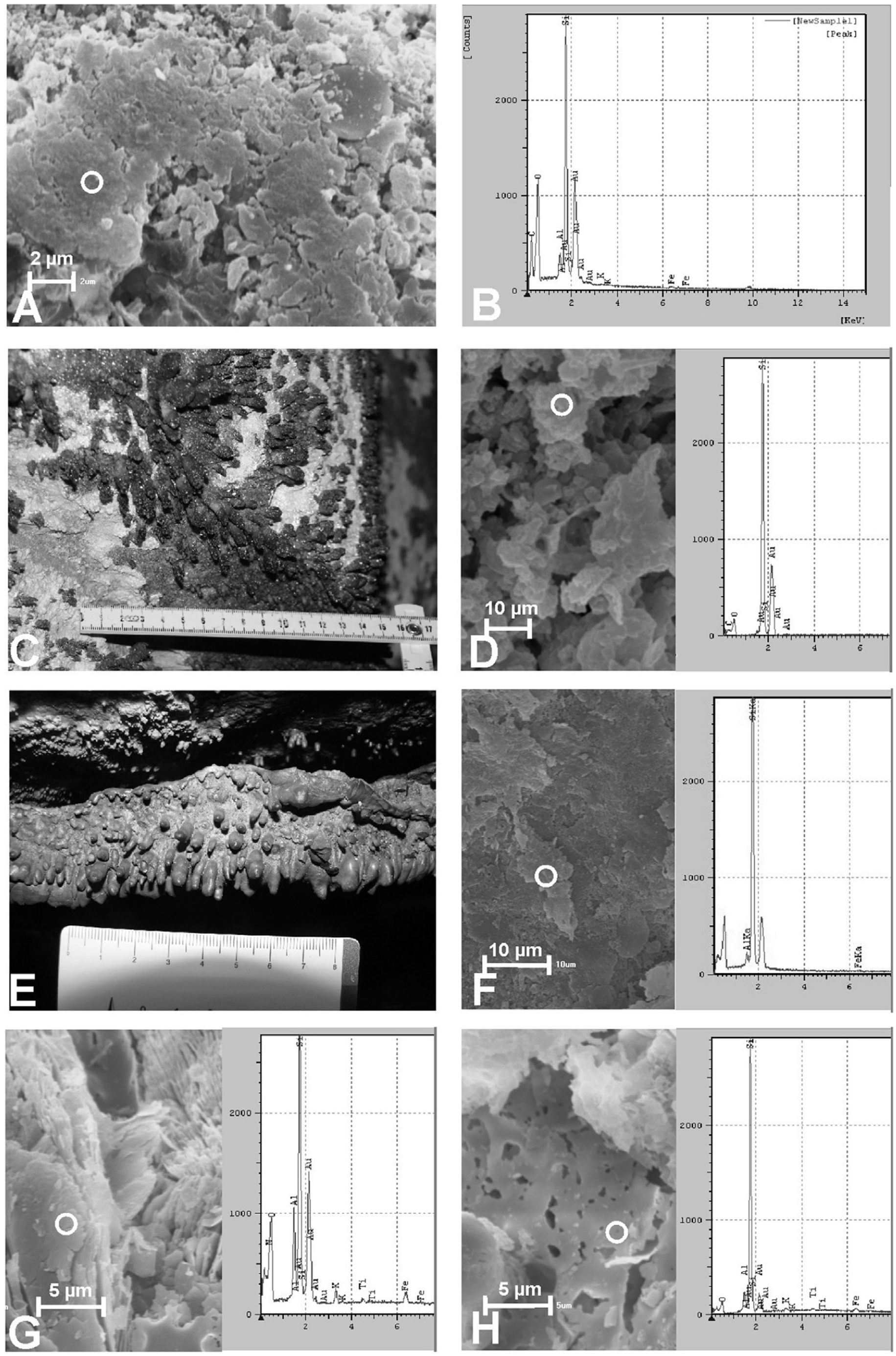

Fig. 10. Three samples from the Chaminé Cave. A: SEM image of sample CC-01, cross section of centimetric speleothem; B: EDS of A indicating that it is cryptocrystalline kaolinite; C: centimetric stalactites (sample CC-04); D: SEM image (left) and EDS (right) of the stalactite in C, indicating that it is silica; E: centimetric speleothems in the wall of the cave (sample CC-05); F: SEM image of speleothem in E (left) and EDS suggesting that it is amorphous silica with some cryptocrystalline kaolinite (right); G: SEM image of the sandstone at the base of the speleothem in E showing large sheets looking partially corroded (left) and EDS indicating that it is illite (right); H: SEM image of sheet pierced by corrosion (left) and EDS indicating that it is illite (the white circles in A, D, F, G and H mark the center of electron beam with 1 μm of radius used in the EDS).

releasing of quartz grains and their subsequent removal by mechanical erosion. This is similar to the concept of 'arenisation' as described by Martini (1979) in quartzites and afterward expanded by Young et al. (2009) and Wray (2013). In its original concept, the arenisation would involve the release of quartz grains by slow corrosion of its edges. In the Furnas Formation the release of quartz grains is mainly due to relatively more rapid corrosion of the kaolinite cement.

Melo and Giannini (2007) summarized studies related to the dissolution conditions of kaolinite, whose main reaction in acid medium is expressed in Schott and Oelkers (1995):

$$AlSiO_{5/2}(OH)_2 + 3H^+ \Leftrightarrow Al^{3+} + (SiO_2 \cdot nH_2O) + (5/2 - n)H_2O \quad (1)$$

Although the sampling and observations of the kaolinite dissolution processes in the Furnas Formation have been carried

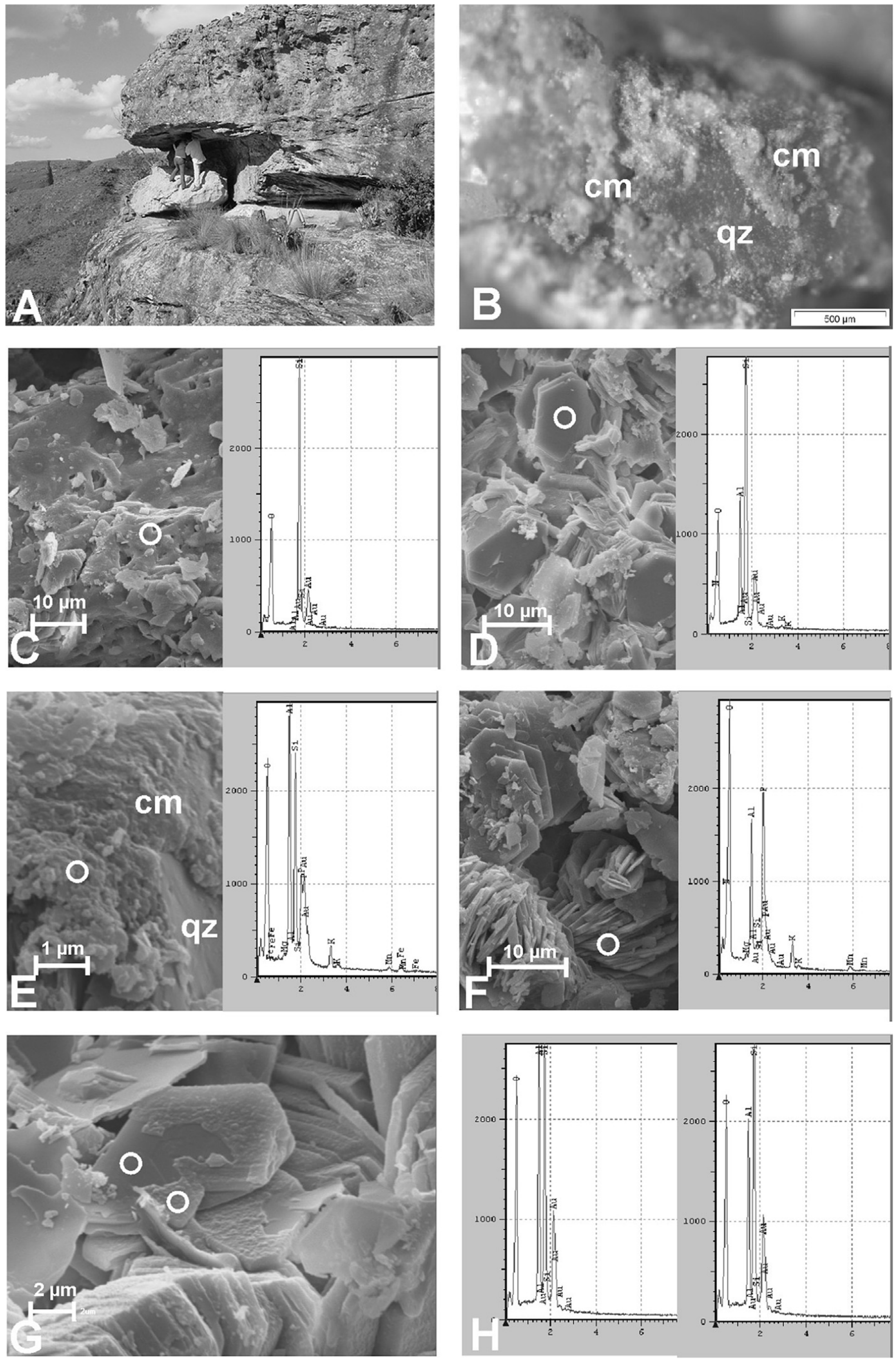

Fig. 11. Sample FU-35. A: Lapa Ponciano, natural shelter in the Guartelá Canyon; B: stereo microscope image of the sandstone at the shelter, showing quartz grain (qz) covered by light cement (cm); C: SEM image and EDS of corroded quartz grain in B; D: SEM image and EDS of mesodiagenetic kaolinite booklets in the light cement in B; E: SEM image of quartz grain (qz) covered by cryptocrystalline cement (cm) (left) and EDS of the cement (right); F: SEM image and EDS of the light cement in B showing unidentified mineral containing Al, P, K, Mg, Mn, Si, possibly the same cryptocrystalline mineral seen in E; G: SEM image of mesodiagenetic kaolinite covered by thin rough membrane; H: EDS of the kaolinite (left) and of the rough membrane (right) in G, indicating that the latter is composed of silica (the white circles in C, D, E, F and G mark the center of electron beam with 1 µm of radius used in the EDS).

out on the ground surface, it is expected that the same processes also occur in depth, provided that the H^+ ion is present. Wide variation in the production of groundwater from deep-drilled wells (Maack, 1970; Melo et al., 2011) and the observation of voids in these wells (Melo et al., 2011) indicate that the Furnas Formation is a karst aquifer. The output of sand in groundwater sources (Melo et al., 2000) indicates underground sandstone quartz grains release and transport.

Acids resulting from bacterial activity can have a noticeable influence on the efficiency of this reaction (McFarlane and Bowden, 1992; Busche and Sponholz, 1992; Maurice et al., 2001; Büdel et al., 2004; Turkington and Paradise, 2005; Cama and Ganor, 2006; Aubrecht et al., 2008; Wray, 2011). The rock cement and surface incrustations of poorly crystallized (cryptocrystalline) kaolinite (massive or booklets up to 10 µm in SEM images) are interpreted in this paper, as in Melo and Giannini (2007) as resulting from

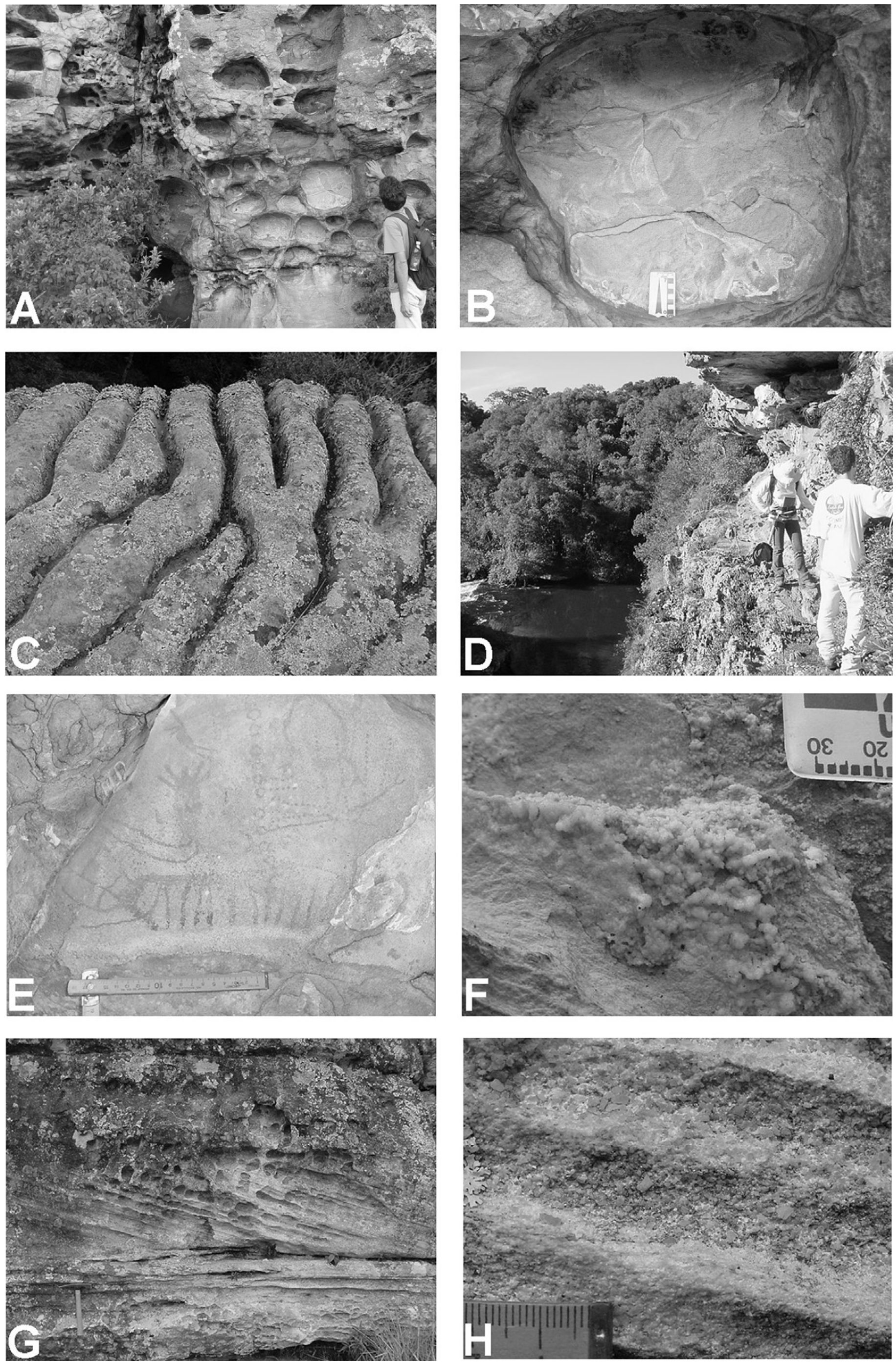

Fig. 12. Some other examples of surface landforms resulting from the dissolution of minerals in the Furnas Formation sandstones. A: rock wall with alveoli locally with structural control (local FU-30); B: detail of A showing exfoliations and kaolinite incrustations on the inner surface of the alveolus; C: runnels (or *karren*) in sandstone (local FU-36); D: archaeological site in rock shelter (local SU-07); E: rock painting degraded by surface exfoliation due to the dissolution of the kaolinite (local GU-09); F: incrustation of kaolinite in sheltered rocky surface (local SU-05); G: rock wall with differential erosion partly controlled by sedimentary structure (local SU-07); H: detail of G showing excavation of coarser strata of the sandstone, where the kaolinitic cement is more abundant.

telodiagenetic phenomena involving reprecipitation of mesodiagenetic well crystallized kaolinite dissolved by weathering processes.

Dissolution of illite, the occurrence of which is indicated by the results of this paper, has been experimentally studied (Hugues et al., 1989; Köhler et al., 2003), especially under conditions simulating hydrocarbon reservoir situations. However, there is a lack of studies correlating this specific dissolution with the geological behavior of aquifers and/or with surface features.

Besides kaolinite, the dissolution and reprecipitation of quartz evidenced in the crusts and speleothems of this study, including a telodiagenetic phase of botryoidal opal formation, have already been described in other studies on the Furnas Formation sandstones (De Ros, 1998; Melo and Giannini, 2007).

Table 2
Relative time succession of the major diagenetic and weathering processes of the Furnas Formation sandstones (see text for a full description). Crosses represent relative time occurrence of the processes in each diagenetic stage.

Process	Eodiagenesis	Mesodiagenesis	Telodiagenesis
Mechanical compaction	XXXXXXXXXX		
Syntaxial quartz overgrowth	XXXXXXXXXX	XXXXXXXXXXXX	
Feldspar dissolution	XXXXXXXXXXX		
Formation of well crystallized kaolinite		XXXXXXXXXXXXX	
Formation of well crystallized illite		XXXXXXXXXXXXX	
Quartz corrosion	XXX		XXXXX
Kaolinite dissolution			XXXXXXXXXX
Illite dissolution			XXXXXXXXXX
Arenisation (secondary porosity)			XXXXXXXXX
Formation of poor crystallized kaolinite			XXXXXX
Formation of poor crystallized illite			XXXXXX
Formation of amorphous silica			XXXXXX
Formation of other minerals (Fe-oxides, variscite, alunite supergroup minerals, etc.)			XXX
Exfoliation, incrustation, small speleothems			XXX
Formation of alveoli and other processes of surface dissolution			XXX

Kaolinite and illite are less soluble than carbonates, but much more soluble than quartz. As sandstones with dominant kaolinitic and illite cement, it can be considered that the Furnas Formation tends to develop karstic phenomena more slowly than in carbonate rocks, but faster than in other quartzose rocks.

6. Concluding remarks and recommendations

The studies carried out here show that the mineral dissolution and reprecipitation processes in the Furnas Formation quartz sandstones are important and widespread. These phenomena especially affect the clay diagenetic cement (kaolinite, illite) and its products are preserved and visible in protected sites (caves, natural shelters, sheltered walls). Microforms (grain corrosion) seen in rock samples and meso (speleothems, alveoli, runnels) to macroforms (caves, "furnas") show close relation with clay cement mobilization, indicating that dissolution processes are a main factor in the origin of the landforms.

Some factors directly controlling the dissolution and reprecipitation processes seem to be well known: the nature of the sandstone (texture, fabric, mineralogy, sedimentary structures), brittle structures (faults, fractures), hydraulic gradient associated with the topography in the Devonian Scarp, a humid subtropical climate, rocks and relief antiquity. Other factors still need further clarification, such as the role of the microorganisms and the influence of climatic variation. There is also an insufficient understanding of details of the physical chemistry of transformations involving quartz, feldspars, kaolinite and illite cements and telodiagenetic typical minerals (variscite, alunite supergroup minerals and others).

The existence of a belt of underlying carbonate rocks coinciding with an ancient shear zone in the basement of the Furnas Formation may be locally forcing underground dynamics and increasing karst forms in the overlying sandstones. However karst forms are widespread in the outcropping area of the Furnas Formation even when the substrate rocks are granites, rhyolites and other non-carbonate rocks. A possible underlying karst is an additional factor that locally combines with the other factors (brittle structures, relief, rock texture and cement) for the genesis of the karst features.

Kaolinite as speleothems, reprecipitations and exfoliations is quite well preserved on the rock walls. Sometimes these are degrading rock paintings by prehistoric Indians, suggesting that the features are still active. This indicates that the dissolution and precipitation phenomena responsible for karst features are currently taking place, and thus are not inherited forms due to paleoenvironmental conditions drastically different from those of today. Kaolinite corrosion is the most frequently observed process, indicating that it is faster than the corrosion of quartz grains. Removal of kaolinite results in the phenomenon of arenisation and an increase in secondary porosity, where the release of the framework grains facilitates the collapse of the sandstone and further mechanical erosion.

Although landforms developed on the Furnas Formation rocks have been associated with phenomena interpreted as karstic since the mid-twentieth century (Maack, 1946, 1956), other authors have contested the importance of dissolution processes in the sandstones (Sallun Filho and Karmann, 2007).

Various authors have discussed the concepts of karst and karst relief (Young, 1986; Wray, 1997a,b; Willems, 2000; Young et al., 2009; Wray, 2013). Despite the controversy about the phenomena and processes involved in the conceptualization of karst, it seems wise to recognize that the quartz sandstones of the Furnas Formation exhibit phenomena of dissolution and recrystallization which, if they do not occur at the same rate as those observed in carbonate rocks, end up with similar surface and underground features and water dynamics. Because the dissolution mainly affects the kaolinitic cement, the Furnas Formation sandstones are eroded faster than other quartzose rocks, such as the quartzites studied in Venezuela (Doerr, 1999) and sandstones in Australia (Young, 1986).

These typical features involve various consequences: exceptional landforms constituting natural heritage (geological and speleological categories), requiring proper management; risk of land subsidence phenomena; risk of contamination and depletion of the Furnas Aquifer, which has characteristics of fractured and karst aquifer.

The cities of Ponta Grossa and Carambeí, in the Campos Gerais region, State of Paraná, have increased the exploitation of the Furnas Aquifer water for industrial, agricultural and public supply (Melo, 2009; Melo et al., 2011). Given the characteristics and increasing use of the aquifer, public policies, including specific legislation aimed at sustainable management of water resources, natural heritage and geo-environmental risks in the region, are urgently needed.

Acknowledgments

To the CNPq – Conselho Nacional de Desenvolvimento Científico e Tecnológico (process n° 477608/07-8) – that funded the research and to Michael Alan Watkins, for the English revision.

References

Assine, M.L., 1996. Aspectos da Estratigrafia das Seqüências Pré-Carboníferas da Bacia do Paraná no Brasil. Ph. D. thesis. Instituto de Geociências da Universidade de São Paulo.

Assine, M.L., Soares, P.C., Milani, É.J., 1994. Seqüências tectono-sedimentares mesopaleozóicas da Bacia do Paraná, Sul do Brasil. Rev. Bras. Geociências 24 (2), 77–89.

Aubrecht, R., Brewer-Carías, C., Šmída, B., Audy, M., Kováčic, L., 2008. Anatomy of biologically mediated opal speleothems in the world's largest sandstone cave: Cueva Charles Brewer, Chimantá Plateau, Venezuela. Sediment. Geol. 203, 181–195.

Bergamaschi, S., 1999. Análise Estratigráfica do Siluro-Devoniano (Formações Furnas e Ponta Grossa) da Sub-Bacia de Apucarana, Bacia do Paraná, Brasil. Ph.D. thesis. Instituto de Geociências da Universidade de São Paulo.

Bigarella, J.J., Becker, R.D., Santos, G.F., 1994. Estrutura e Origem das Paisagens Tropicais e Subtropicais, vol. 1. Editora da UFSC, Florianópolis.

Biondi, J.C., Cava, L.T., Soares, P.C., 1989. Mapa Geológico do Estado do Paraná – Escala 1:650.000. DNPM/Mineropar, Curitiba.

Büdel, B., Weber, B., Kühl, M., Pfanz, H., Sültemeyer, D., Wessels, D., 2004. Reshaping of sandstone surfaces by cryptoendolithic cyanobacteria: bioalkalization causes chemical weathering in arid landscapes. Geobiology 2, 261–268.

Busche, D., Sponholz, B., 1992. Morphological and micomorphological aspects of sandstone karst of eastern Niger. Z. Für Geomorphol. 1–18. Vol. Suppl.-Bd. 85.

Cama, J., Ganor, J., 2006. The effects of organic acids on the dissolution of silicate minerals: a case study of oxalate catalysis of kaolinite dissolution. Geochim. Cosmochim. Acta 70, 2191–2209.

De Ros, L.F., 1998. Heterogeneous generation and evolution of diagenetic quartzarenites in the Silurian–Devonian Furnas Formation of the Paraná Basin, southern Brazil. Sediment. Geol. 116 (1/2), 99–128.

Doerr, S.H., 1999. Karst-like landforms and hydrology in quartzites of the Venezuelan Guyana shield: pseudokarst or 'real' karst? Z. Für Geomorphol. 43 (1), 1–17.

Hugues, C.R., Davey, R.C., Curtis, C.D., 1989. Chemical reactivity of some reservoir illites: implications for petroleum production. Clay Miner. 24, 445–458.

Köhler, S.J., Dufaud, F., Oelkers, E.H., 2003. An experimental study of illite dissolution kinetics as a function of pH from 1.4 to 12.4 and temperature from 5 to 50°C. Geochim. Cosmochim. Acta 67 (19), 3583–3594.

Lobato, G., Borghi, L., 2005. Análise estratigráfica da Formação Furnas (Devoniano Inferior) em afloramentos da borda leste da Bacia do Paraná. In: Proceedings 3º Congresso Brasileiro de P&D em Petróleo e Gás, Salvador, pp. 1–6.

Maack, R., 1946. Geologia e geografia da região de Vila Velha e considerações sobre a glaciação carbonífera do Brasil. Arq. do Mus. Parana. 5, 1–305.

Maack, R., 1948. Notas preliminares sobre clima, solos e vegetação do Estado do Paraná. Arq. Biol. Tecnol. 2, 102–200.

Maack, R., 1956. Fenômenos carstiformes de natureza climática e estrutural de arenitos do Estado do Paraná. Arq. Biol. Tecnol. 11, 151–162.

Maack, R., 1970. Notas preliminares sobre as águas do sub-solo da Bacia do Paraná-Uruguai. Comissão Interestadual da Bacia do Paraná-Uruguai, Curitiba.

Martini, J.E.J., 1979. Karst in black reef quartzite near kaapsehoop, eastern transvaal. Ann. South Afr. Geol. Surv. 13, 115–128.

Maurice, P.A., Vierkorn, M.A., Hersman, L.E., Fulghum, J.E., Ferryman, A., 2001. Enhancement of kaolinite dissolution by an aerobic *Pseudomonas mendocina* bacterium. Geomicrobiol. J. 18 (1), 21–35.

McFarlane, M.J., Bowden, D.J., 1992. Mobilization of aluminium in the weathering profiles of the African surface in Malawi. Earth Surf. Process. Landforms 17, 789–805.

Melo, M.S., 2009. Aqüífero Furnas: urgência na proteção de mananciais subterrâneos em Ponta Grossa, PR. In: Proceedings 21º Seminário Internacional Experiências de Agendas 21-Desafios do Nosso Tempo, Curitiba, p. 11.

Melo, M.S., Giannini, P.C.F., 2007. Sandstone dissolution landforms in the Furnas Formation, southern Brazil. Earth Surf. Process. Landforms 32, 2149–2164.

Melo, M.S., Giannini, P.C.F., Pessenda, L.C.R., 2000. Gênese e evolução da Lagoa Dourada, Ponta Grossa, PR. Rev. do Inst. Geológico 21 (1/2), 17–31.

Melo, M.S., Giannini, P.C.F., Sayeg, I.J., 1999. Kaolinitic clay in the furnas Sandstone, devonian of the paraná Basin, southern Brazil. Acta Microsc. 8(A), 37–38.

Melo, M.S., Guimarães, G.B., Pontes, H.S., Massuqueto, L.L., Pigurim, I., Bagatim, H.Q., Giannini, P.C.F., 2011. Carste em rochas não-carbonáticas: o exemplo dos arenitos da Formação Furnas, Campos Gerais do Paraná/Brasil e implicações para a região. Espeleo Tema 22 (10), 81–97.

Melo, M.S., Lopes, M.C., Boska, M.A., 2005. Furna do Buraco do Padre, Formação Furnas, PR – feições de erosão subterrânea em arenitos devonianos da Bacia do Paraná. In: Winge, M., Schobbenhaus, C., Berbert-Born, M., Queiroz, E.T., Campos, D.A. (Eds.), Sítios Geológicos e Paleontológicos do Brasil, CPRM, Brasília, vol. II, pp. 47–57.

Mineropar – Minerais do Paraná, 2006. Cartas geológicas do Estado do Paraná – Escala 1:250.000. Mineropar, Curitiba.

Ramos, A.N., Formoso, M.L.L., 1975. Argilominerais das rochas sedimentares da Bacia do Paraná. Ciência Técnica Petróleo Seção Exploração Petróleo 9, 1–46.

Sallun Filho, W., Karmann, I., 2007. Dolinas em arenitos da Bacia do Paraná: evidências de carste subjacente em Jardim (MS) e Ponta Grossa (PR). Rev. Bras. Geociências 37 (3), 551–564.

Schott, J., Oelkers, E.H., 1995. Dissolution and crystallization rates of silicate minerals as a function of chemical affinity. Pure Appl. Chem. 67 (6), 903–910.

Soares, O., 1989. Furnas dos Campos Gerais, Paraná. Scientia et Labor. Editora da UFPR, Série Didática, Curitiba.

Turkington, A.V., Paradise, T.R., 2005. Sandstone weathering: a century of research and innovation. Geomorphology 67, 229–253.

Welton, J.E., 1984. SEM Petrology Atlas. The American Association of Petroleum Geologists, Tulsa, Oklahoma (Methods in exploration series).

Willems, L., 2000. Phénomènes karstiques en roches silicatées non carbonatées – Cas des grès, des micachistes, des gneiss et des granites en Afrique sahélienne et équatoriale. Ph.D. thesis. Université de Liège.

Willems, L., Compère, P., Hatert, F., Pouclet, A., Vicat, J.P., Ek, C., Bouvain, F., 2002. Karst in granitic rocks, South Cameroon: cave genesis and silica and taranakite speleothems. Terra Nova 14 (5), 355–362.

Wray, R.A.L., 1997a. A global review of solutional weathering forms on quartz sandstones. Earth Sci. Rev. 42, 137–160.

Wray, R.A.L., 1997b. Quartzite dissolution: karst or pseudokarst? Cave Karst Sci. 24 (2), 81–86.

Wray, R.A.L., 2011. Alunite formation within silica stalactites from the Sydney Region, South-eastern Australia. Int. J. Speleol. 40 (2), 31–38.

Wray, R.A.L., 2013. Solutional weathering and karstic landscapes on quartz sandstones and quartzite. In: Frumkin, A. (Ed.), Treatise on Geomporphology, Karst Geomorphology, vol. 6. Academic Press, San Diego, pp. 463–483.

Young, R.W., 1986. Tower karst in sandstone: bungle bungle massif, northwestern Australia. Z. Für Geomorphol. 30 (2), 189–202.

Young, R.W., Wray, R.A.L., Young, A.R.M., 2009. Sandstone Landforms. Cambridge University Press, Cambridge.

Zalán, P.V., Wolff, S., Conceição, J.C.J., Marques, A., Astolfi, M.A.M., Vieira, I.S., Appi, V.T., Zanotto, O.A., 1991. Bacia do Paraná. In: Gabaglia, G.R., Milani, É.J. (Eds.), Origem e Evolução de Bacias Sedimentares. Petrobrás, Rio de Janeiro, pp. 135–168.